Orbital and spin-orbit magnetic susceptibilities in face-centred cubic transition metals and noble metals

Orbital and spin–orbit magnetic susceptibilities in face-centred cubic transition metals and noble metals

M Yasui†, T Takahashi† and J Callaway‡

† Department of Electrical Engineering and Computer Science, Yamanashi University, Kofu 400, Japan
‡ Department of Physics and Astronomy, Louisiana State University, Baton Rouge, LA 70803, USA

Abstract. The uniform unenhanced orbital and spin–orbit susceptibilities, χ_o and χ_{so}, respectively, in Ni, Pd and Pt are evaluated by taking numerical extrapolations to $q = 0$ of our previous expressions for the wavenumber (q)-dependent orbital and spin–orbit susceptibilities, $\chi_o(q)$ and $\chi_{so}(q)$, respectively. The wavefunctions and energies required in these calculations are obtained from self-consistent relativistic APW band calculations in the relativistic local-density approximation. From a study of trends in χ_o and χ_{so} with the number of conduction electrons per atom ratio for FCC 3d, 4d and 5d metal series, χ_o and χ_{so} in Rh, Ir, Cu, Ag and Au are estimated in the rigid-band assumption with reasonable corrections. For all these metals, our values of $\chi_o + \chi_{so}$ show good agreement with empirical values. By using previously reported theoretical values of the enhanced spin susceptibility $I\chi_s$, the total susceptibility $\chi = I\chi_s + (\chi_o + \chi_{so})$ is estimated and compared with observed results for these metals.

1. Introduction

The spin contribution to the magnetic susceptibility in transition metals has been studied more extensively than the orbital contribution for many years and its discussion is becoming more and more quantitative; within the local-density theory of exchange and correlation [1], the enhanced spin susceptibility has been calculated without any adjustable parameter for paramagnetic [2–5] and ferromagnetic [6, 7] transition metals. In order to discuss agreement or disagreement between theory and experiment, however, we need to study the orbital contribution to the magnetic susceptibility. In transition metals, the orbital contribution is not always negligible; the orbital susceptibility is larger than the spin susceptibility in some transition metals. For the quantitative study of the magnetic susceptibility in transition metals, the orbital susceptibility including the core diamagnetic susceptibility should be evaluated as correctly as possible. Since the enhancement effect is assumed to be not very significant in regard to orbital magnetism [8–10], we may treat the problem within the single-electron model for the present.

We know a correct formula of the uniform unenhanced orbital susceptibility χ_{orb} for Bloch electrons [11], but it is too complicated to be evaluated quantitatively. No one has done this properly for transition metals. This complicated formula, however, is

derived from the wavenumber (q)-dependent orbital susceptibility $\chi_{orb}(q)$ [12] by taking the limit $q \to 0$. One may, therefore, suppose that reasonably correct values of χ_{orb} may be obtained from a numerical extrapolation of $\chi_{orb}(q)$ to $q = 0$. This simple and practical scheme of calculation has been found successful in obtaining reliable values of χ_{orb} in 3d transition metals [13–15].

The computational scheme for χ_{orb} based on $\chi_{orb}(q)$ is inadequate for 4d and 5d transition metals. Relativistic effects such as the spin–orbit coupling should be taken into account in these metals, but $\chi_{orb}(q)$ is derived in a non-relativistic manner. Relativistic expressions for the magnetic susceptibility are obtained from the Fourier components of the Dirac current induced by the applied external field. Yasui and Shimizu [16] have derived an expression for the generalized susceptibility $\chi_{zz}(q, q)$ (q is the wavenumber vector) to discuss the uniform susceptibility $\chi_{zz}(0, 0)$, while Misra and Callaway [17] have derived one for $\chi_{zz}(G + q, q)$ ($G \neq 0$ is a reciprocal-lattice vector) to discuss the induced-moment form factor $\chi_{zz}(G, 0)$. A relativistic formula for the wavenumber-dependent susceptibility $\chi(q)$ is obtained from $\chi_{zz}(q, q)$ by choosing q as $q = (0, q, 0)$, for instance, and is expressed as the sum of three terms: the wavenumber-dependent spin, spin–orbit and orbital susceptibilities, $\chi_s(q)$, $\chi_{so}(q)$ and $\chi_o(q)$, respectively [16]. The uniform unenhanced spin, spin–orbit and orbital susceptibilities, χ_s, χ_{so} and χ_o, are obtained by taking the limit $q \to 0$ of $\chi_s(q)$, $\chi_{so}(q)$ and $\chi_o(q)$, respectively. In a previous paper [18], we have calculated χ_o and χ_{so} in typical BCC transition metals, V, Nb and W, by taking numerical extrapolations of $\chi_o(q)$ and $\chi_{so}(q)$ to $q = 0$, and discussed the relativistic effects in BCC 3d, 4d and 5d transition metals. This time, we make similar calculations for typical FCC transition metals, Ni, Pd and Pt.

Although Ni is ferromagnetic at low temperatures, its paramagnetic properties at higher temperatures are also of interest. Fortunately, the orbital contribution to the magnetic susceptibility is expected to be almost temperature independent, so that a correct evaluation of χ_o and χ_{so} in paramagnetic Ni is possible. On the other hand, Pd and Pt are of interest because of their large paramagnetic susceptibilities and associated magnetic properties. Since Ni, Pd and Pt are metals with nearly filled d bands, the orbital contribution to the magnetic susceptibility is expected to be small and has been neglected in most theoretical and experimental studies. We must, however, examine to what extent χ_o and χ_{so} are actually small in these metals.

The method of calculation of χ_o and χ_{so} is explained briefly in section 2. Calculated results are shown and discussed in section 3, and concluding remarks are given in section 4.

2. Method of calculation

By using positive energy solutions (four-component Bloch function $|i\rangle$ and its energy ε_i, where i designates a set of indices including the wavevector, band index and spin direction) of the Dirac equation for an electron in a periodic potential, $\chi_o(q)$ and $\chi_{so}(q)$ are written as [16]

$$\chi_o(q) = q^{-2}\mu_B^2[A(q) - A(0)] \tag{1}$$

and

$$\chi_{so}(q) = q^{-1}\mu_B^2 B(q) \tag{2}$$

where

$$A(q) = \frac{8}{V} \sum_j \sum_i \Theta_{ji} \left| \langle j| \exp(iqy) \, \beta \, \frac{\partial}{\partial x} |i\rangle \right|^2 \tag{3}$$

and

$$B(q) = \frac{8}{V} \sum_j \sum_i \Theta_{ji} \operatorname{Re} \left(\langle j| \exp(iqy) \beta \Sigma_z |i\rangle^* \langle j| \exp(iqy) \, \beta \, \frac{\partial}{\partial x} |i\rangle \right). \tag{4}$$

In the above expressions β is one of the usual 4×4 Dirac matrices, Σ_z is one of the 4×4 spin matrices, V is the volume of the system, μ_B is the Bohr magneton, Re( ) means the real part, and $\Theta_{ji} = (1 - \theta_j)\theta_i/(\varepsilon_j - \varepsilon_i)$ where θ_i is a step function $\theta(\varepsilon_F - \varepsilon_i)$ $(\theta(x \geqslant 0) = 1, \theta(x < 0) = 0)$ with the Fermi level ε_F. These expressions are valid within the order of c^{-2}, where c is the speed of light. In the limit $c \to \infty$, $\chi_o(q)$ reduces to $\chi_{orb}(q)$, while $\chi_{so}(q)$ reduces to 0 and represents explicitly a relativistic correction to the susceptibility. It should be noted that the core diamagnetic contribution to the susceptibility is already included in $\chi_o(q) + \chi_{so}(q)$ as shown by Oh *et al* [19] in the non-relativistic case.

The analytical formulae for χ_o and χ_{so} are obtained by taking the limit $q \to 0$ of $\chi_o(q)$ and $\chi_{so}(q)$, respectively, but are very complex to use for numerical calculations [20]. Therefore, we evaluate χ_o and χ_{so} as follows. Since $A(q)$ and $B(q)$ have expansions as $A(q) = a_0 + a_2 q^2 + a_4 q^4 + \ldots$ and $B(q) = b_1 q + b_3 q^3 + b_5 q^5 + \ldots$ at $q = 0$, χ_o and χ_{so} are given by $\chi_o = \mu_B^2 a_2$ and $\chi_{so} = \mu_B^2 b_1$. The expansion coefficients a_2 and b_1 are determined by calculating $A(q)$ and $B(q)$ at several small values of q and fitting the above expansion formulae to these calculated values. It is important to obtain the q-dependences of $A(q)$ and $B(q)$ as correctly as possible and this is attainable if we carry out the reciprocal space summations in (3) and (4) by the tetrahedron method [21–24] based on a mesh of at least 16 divisions along the ΓX lines in the Brillouin zone (505 equally spaced mesh points in one forty-eighth of the Brillouin zone). As for small values of q, four values q_2, q_5, q_8 and q_{11} are assumed, where $q_n = (2\pi/a)\sqrt{n/512}$ and a is the lattice constant. Computational details have been explained elsewhere [13].

3. Calculated results and discussion

3.1. Self-consistent energy band calculations

Wavefunctions and energies required in the calculation of χ_o and χ_{so} are obtained from self-consistent relativistic APW band calculations in the relativistic local-density approximation. The outline of these band calculations is as follows. A muffin-tin-type crystal potential as proposed by Janak [25] was employed. The relativistic exchange–correlation potential given by MacDonald *et al* [5, 26] was used. The lattice constant was assumed to be 6.644 au in Ni [27], 7.340 au in Pd [5] and 7.398 au in Pt [5]. The usual relativistic APW method [28] was used to solve the Dirac equation by adopting about 35 reciprocal-lattice vectors. The crystal potentials of Ni and Pd, tabulated by Moruzzi *et al* [29], were used as starting potentials for our self-consistent calculations. As for Pt, our starting potential was obtained simply from overlapping atomic potentials of Pt, as calculated by Herman and Skillman [30]. For conduction electrons, wavefunctions and energies were calculated on 89 equally spaced mesh points in one forty-eighth of the Brillouin zone. The density of states and the electron density were calculated by using the tetrahedron method [21–24] with these mesh points. On the other hand, for core
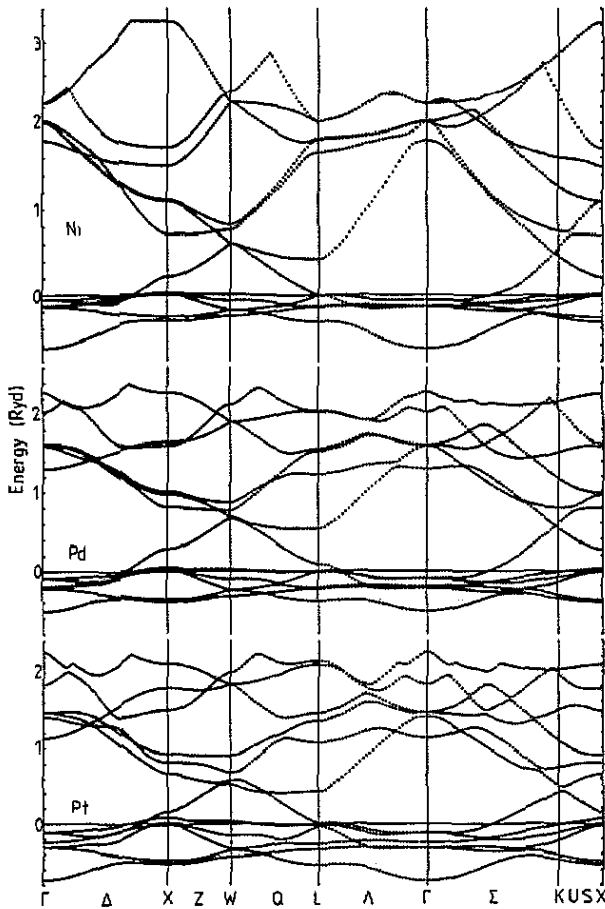
Figure 1. Self-consistent energies in the lowest 12 bands plotted along some lines of symmetry. The energies are relative to the Fermi level shown by the horizontal lines.

electrons, we neglected the wavevector dependences of wavefunctions and energies. Core levels were obtained from the condition that the wavefunctions behave as atomic functions outside the APW sphere. The electron density was calculated from these atomic functions which were normalized within the Wigner–Seitz sphere. The cycle of the self-consistent calculation was finished when the difference between successive potentials became less than 0.01%, i.e. $\max|(v_{N+1} - v_N)/v_N| < 10^{-4}$, and v_N thus obtained was used in the subsequent calculation. The energies of conduction states converged to better than 0.3 mRyd. As for core states, seven or more significant figures of energy values were found to remain unchanged during the final few cycles.

In figure 1, the self-consistent energies in the lowest 12 bands for Ni, Pd and Pt are plotted along some lines of symmetry. The horizontal lines show the Fermi level, respective values of which are 0.5165 Ryd, 0.4209 Ryd and 0.5249 Ryd for Ni, Pd and Pt. The spin–orbit coupling effect is weak in Ni, rather strong in Pd and considerably stronger in Pt. We take into account these 12 bands in the calculation of χ_0 and χ_{so}. In figure 2, the densities of states in the lowest six bands for Ni, Pd and Pt are shown and their respective values at the Fermi level, indicated by the vertical lines, are 60.3 states
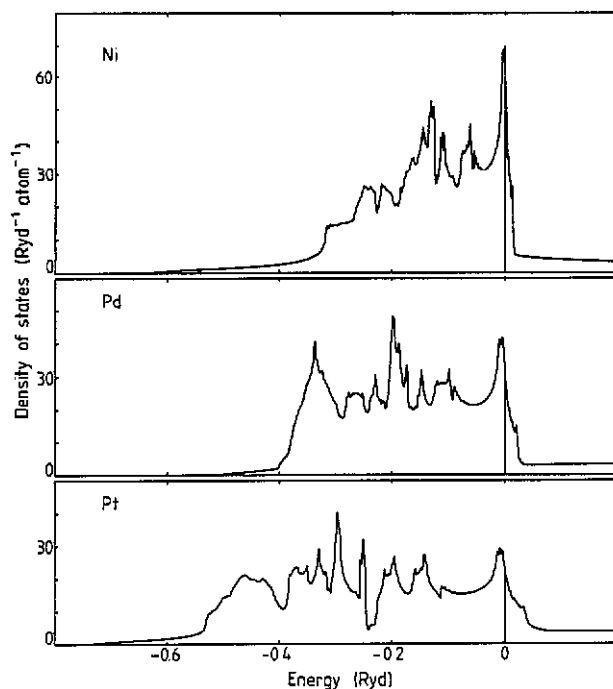
Figure 2. Density-of-states curves for Ni, Pd and Pt. The energies are relative to the Fermi level shown by the vertical lines.

Ryd^{-1}/atom, 31.3 states Ryd^{-1}/atom and 23.1 states Ryd^{-1}/atom. The broadening of the d bandwidth in going from Ni to Pt can be seen explicitly. The calculated energy band structures (lower six bands and higher six bands) shown in figure 1 do not differ in any significant way from previous calculations [31–33] and we show them only to facilitate the discussion in the remainder of this paper. Koelling and MacDonald [34] have discussed in detail the relativistic effects occurring in transition metals, and Bacalis *et al* [35] the effects of various approximations used in performing the APW band calculations for transition metals.

Our self-consistent core levels are shown in table 1. We have adopted the same lattice constants and the same relativistic exchange–correlation potential as those used by MacDonald *et al* [5], but our energies for Pd and Pt differ slightly from theirs. This may come from the different conditions under which the core levels are determined. In the calculation of χ_o and χ_{so}, only the core states higher in energy than -10 Ryd are taken into account and others are neglected because they lie far from the conduction bands. Our self-consistent potentials v_N actually produce narrow bands around the related atomic core levels. Their widths, shown in table 1, however, are so narrow that our treatment of core states is valid.

3.2. Calculated results of χ_o and χ_{so}

By making use of the wavefunctions and energies obtained above, χ_o and χ_{so} are calculated in the manner explained in section 2. In this paper, all susceptibilities are given in units of 10^{-6} emu mol^{-1}.

Table 1. Core levels in Ni, Pd and Pt. These energies have been determined by assuming that wavefunctions behave as atomic functions outside the APW sphere. The values in parentheses show the width of the related actual core band. All energies are in Ryd.

(nlj)	Energy (Ryd)		
	Ni	Pd	Pt
$(1s\frac{1}{2})$	−599.3315	−1764.6497	−5712.9437
$(2s\frac{1}{2})$	−70.6923	−257.4756	−1003.3032
$(2p\frac{1}{2})$	−61.6556	−239.1440	−962.2734
$(2p\frac{3}{2})$	−60.3789	−227.5315	−836.9126
$(3s\frac{1}{2})$	−6.9685 (0.0036)	−45.9720	−235.1624
$(3p\frac{1}{2})$	−4.2130 (0.0090)	−38.6838	−216.6254
$(3p\frac{3}{2})$	−4.0515 (0.0135)	−36.6577	−189.0410
$(3d\frac{3}{2})$		−23.6472	−158.0145
$(3d\frac{5}{2})$		−23.2413	−152.0362
$(4s\frac{1}{2})$		−5.7185 (0.0055)	−49.8536
$(4p\frac{1}{2})$		−3.4511 (0.0149)	−41.9697
$(4p\frac{3}{2})$		−3.1205 (0.0260)	−35.3785
$(4d\frac{3}{2})$			−22.4127
$(4d\frac{5}{2})$			−21.1811
$(4f\frac{5}{2})$			−4.5462 (0.0001)
$(4f\frac{7}{2})$			−4.2924 (0.0004)
$(5s\frac{1}{2})$			−6.6672 (0.0034)
$(5p\frac{1}{2})$			−4.1383 (0.0105)
$(5p\frac{3}{2})$			−3.0407 (0.0354)

3.2.1. Trends in χ_o and χ_{so} for FCC d-band metals. In order to facilitate the presentation of our results, we first show the trends in χ_o and χ_{so} with the ratio e/a of the number of conduction electrons to atoms. Under the assumption of rigid bands, the variations in χ_o and χ_{so} with e/a are calculated for the FCC 3d, 4d and 5d metal series by using the wavefunctions and energies of Ni, Pd and Pt, respectively, and by varying the Fermi level. These results are shown in figure 3 and table 2.

Except for fine structure, the general features of the χ_o versus e/a curve for the FCC 3d, 4d and 5d metal series are similar to the previous results for the respective BCC series [18]. As expected from the factor $(1 - \theta_j)\theta_i$ in Θ_{ji} of (3), each χ_o versus e/a curve has large values over the middle range of e/a, where the Fermi level lies in the middle of the d band and there are so many states which can be combined by the factor that the values of χ_o become large. Another factor $1/(\varepsilon_j - \varepsilon_i)$ in Θ_{ji} of (3) makes the values of χ_o large when many states combined by the former factor are distributed in a narrow energy range. This situation is so well realized in the 3d series that the heights of the χ_o versus e/a curves for the 3d series are considerably larger than those for the 4d and 5d series. Because of the latter factor, we can roughly assume that χ_o is proportional to the inverse of the d bandwidth W_d, i.e. $\chi_o \propto 1/W_d$. Figure 3 shows that the heights of the χ_o versus e/a curves decrease as one goes from the 3d series to the 5d series. This result can be understood from the relation $\chi_o \propto 1/W_d$ and our observation that $W_d(\text{Ni}) < W_d(\text{Pd}) < W_d(\text{Pt})$ as shown in figure 2. Although the χ_o-values are positive and large over the wide middle range of e/a, they are small, positively or negatively, near the ends of each series. That the contributions of χ_o to the total susceptibilities in
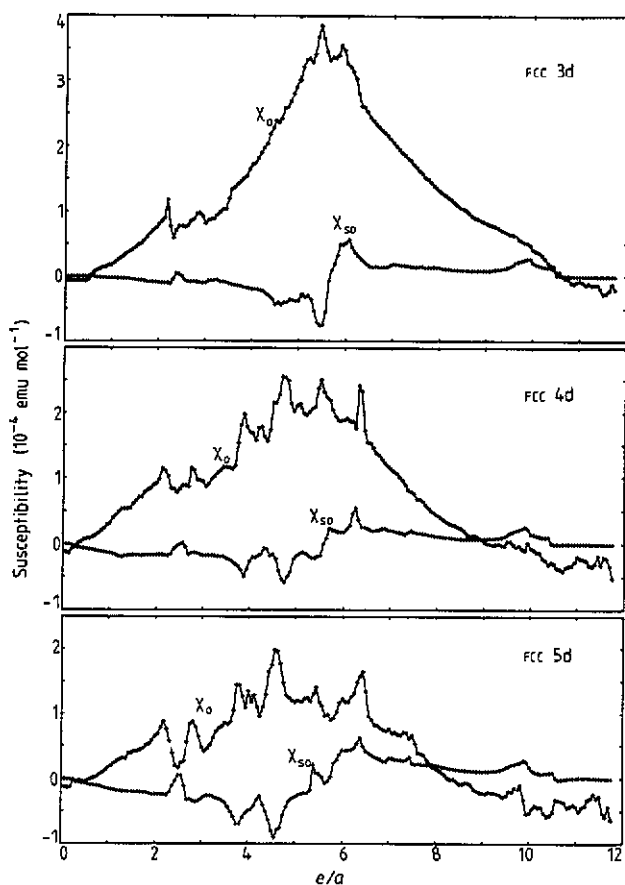
Figure 3. Trends in χ_o and χ_{so} with e/a (the number of conduction electrons per atom). The results for the 3d, 4d and 5d series are calculated by using the band structures of Ni, Pd and Pt, respectively, and by varying the Fermi level. χ_o and χ_{so} for selected values of e/a are listed in table 2.

Ni, Pd and Pt are minor is thus understood. The diamagnetic character of χ_o is explicit for $e/a = 11$, i.e. for noble metals, and is noticeable over a wide upper range of e/a in the 5d series.

As seen from figure 3, three χ_{so} versus e/a curves are mutually very similar. In particular, χ_{so}-values are negative at smaller values of e/a and positive at larger values of e/a. This characteristic has been found also in our previous results of χ_{so} for the BCC 3d, 4d and 5d series [18]. MacDonald [36] has found a similar characteristic in the g-shifts of transition metals; the g-shifts tend to be negative towards the bottom of the d band and positive towards the top of the d band in all cases of BCC, FCC and HCP structures. Following Koelling and MacDonald [34], this characteristic in the g-shifts comes from the fact that, when spin–orbit coupling is included, eigenstates towards the bottom of the d band tend to have spin and orbital angular momentum in opposite directions while those towards the top of the band tend to have these directions more parallel. Probably, this fact has caused the characteristic in the χ_{so} versus e/a curves mentioned above, too.

Since χ_{so} is an explicit relativistic correction to the susceptibility, an increase in the absolute values of χ_{so} is expected in going from the 3d series to the 5d series. On the

Table 2. χ_0 and χ_{so} for selected values of e/a (the number of conduction electrons per atom ratio).

	FCC 3d		FCC 4d		FCC 5d	
e/a	χ_0 $(10^{-6}$ emu mol$^{-1})$	χ_{so} $(10^{-6}$ emu mol$^{-1})$	χ_0 $(10^{-6}$ emu mol$^{-1})$	χ_{so} $(10^{-6}$ emu mol$^{-1})$	χ_0 $(10^{-6}$ emu mol$^{-1})$	χ_{so} $(10^{-6}$ emu mol$^{-1})$
3	82	-10	94	-17	48	-31
4	173	-20	171	-27	135	-49
5	301	-38	211	-19	118	-28
6	327	52	189	18	123	43
7	206	19	113	21	77	31
8	131	13	44	12	16	21
9	82	9	4	8	-22	11
10	42	21	-6	15	-53	18
11	-6	0	-19	0	-43	1

other hand, because of the factor $1/(\varepsilon_j - \varepsilon_i)$ in Θ_{ji} of (4), χ_{so} also depends on W_d as $\chi_{so} \propto 1/W_d$. We can see, from figure 1, that the spin–orbit coupling effect is not much stronger in the 4d series than in the 3d series and, from figure 2, that the 4d band is wider than the 3d band. In figure 3, the depths and/or heights of the χ_{so} versus e/a curves for the 4d series are almost the same as those for the 3d series. This result shows that, in the 4d series, the increase in the relativistic correction is nearly compensated by the increase in W_d. In the 5d series, however, the spin–orbit coupling effect is stronger than in the 4d series so that the increase in the relativistic correction more than compensates the increase in W_d. We thus understand the result that the depths and/or heights of the χ_{so} versus e/a curves for the 5d series are larger than those for the 4d series.

3.2.2. χ_o and χ_{so} in Ni, Pd and Pt.

Table 3 shows, for Ni, Pd and Pt, our calculated values of χ_o, χ_{so} and $\chi_c = \chi_o + \chi_{so}$, empirically estimated values $(\chi_c)_{emp}$ of χ_c, previously reported theoretical values of the enhanced spin susceptibility $I\chi_s$, theoretical values of the total susceptibility $\chi = I\chi_s + \chi_c$ and observed values of the total susceptibility χ_{exp}.

Our result $\chi_c = 63$ for Ni is very close to the empirical value $(\chi_c)_{emp} = 59$ [37] estimated as a temperature-independent contribution to the susceptibility in paramagnetic state. The present result $\chi_o = 42$ is very close to our previous non-relativistic result $\chi_{orb} = 44$ [15] which has been obtained with the lattice constant $a = 6.55$ au and $W_d = 0.360$ Ryd (energy difference between X_1 and X_5 levels in the previous non-relativistic band). If we assume that $\chi_{orb} \propto a^2/W_d$ [16], we can estimate a value of χ_{orb} under the present conditions $a = 6.644$ au and $W_d = 0.339$ Ryd (energy difference between X_7^+ and X_6^+ levels in the present relativistic band). This result $\chi_{orb} = 48$ is still close to the present result $\chi_o = 42$. From a small difference between χ_o and χ_{orb}, the relativistic correction in χ_o seems to be small in Ni.

At low temperatures, Ni is ferromagnetic. Its spin-polarized relativistic band structure is very complex [53, 54] and proper evaluations of χ_o and χ_{so} will be difficult. Therefore, we make crude estimations of χ_o and χ_{so} in ferromagnetic Ni by using a rigidly split band model. Our degenerate paramagnetic bands are split rigidly by 0.53 eV with each other so as to produce the magneton number 0.56 [55]. Respective values of χ_o at the new Fermi level in the majority and the minority spin bands are 4 and 34 and those of χ_{so} are 1 and 7. Sums of the contributions from both bands are listed in table 3. The present result $\chi_c = 46$ is closer to the empirical values than our previous result $\chi_{orb} = 27$ [15]. Because of our crude estimation of χ_c and/or a rather small calculated value of the high-field spin susceptibility $I\chi_s$, agreement between theory and experiment is not so good.

As for Pd and Pt, our values of χ_c are close to the empirical values $(\chi_c)_{emp}$. Since Pd and Pt are transition metals with nearly filled d bands, χ_c has been assumed to be small. In fact, χ_c for Pd is very small and is only about 1% of the large observed paramagnetic susceptibility. The orbital contribution to the magnetic susceptibility is negligible in Pd. On the other hand, in Pt, χ_c is negative and its absolute value is about 17% of the observed susceptibility. The orbital contribution to the magnetic susceptibility is not negligibly small in Pt. Unfortunately, as seen from table 3, previous theoretical results for $I\chi_s$ are still not satisfactory for Ni, Pd and Pt, and we cannot discuss the overall agreement or disagreement between theory and experiment for the total susceptibility.

3.2.3. χ_o and χ_{so} in Rh, Ir, Cu, Ag and Au.

Rh and Ir are, respectively, 4d and 5d transition metals of FCC structure. Cu, Ag and Au are noble metals having filled 3d, 4d

Table 3. Calculated values of χ_0, χ_{so} and $\chi_c = \chi_0 + \chi_{so}$, empirically estimated values $(\chi_c)_{emp}$ of χ_c, previously reported theoretical values of the enhanced spin susceptibility $I\chi_s$, theoretical values of the total susceptibility $\chi = I\chi_s + \chi_c$, and observed values of the total susceptibility χ_{exp}.

	χ_0 (10^{-6} emu mol^{-1})	χ_{so} (10^{-6} emu mol^{-1})	χ_c (10^{-6} emu mol^{-1})	$(\chi_c)_{emp}$ (10^{-6} emu mol^{-1})	$I\chi_s$ (10^{-6} emu mol^{-1})	χ (10^{-6} emu mol^{-1})	χ_{exp} (10^{-6} emu mol^{-1})
Ni	42	21	63	59 [37]			113 [38]
							113–118 [39]
Ni[a]	38	8	46	72 [38]	26 [9]	72	129 [45]
				77–82 [39]			110 [46]
					1120 [2]	1129	771 [47]
					329 [3]	338	745 [48]
					410, 680, 770 [4]	419–779	
Pd	−6	15	9	0 [40]	1120, 1220, 1460 [5]	1129–1469	740 [49]
				18 [41]	638 [42]	647	736 [50]
					522 [43]	531	741 [51]
					352 [44]	361	730 [52]
Pt	−53	18	−35	−15 [40]	473 [2]	438	211 [49]
				−13 [41]	130, 150 [5]	95–115	216 [50]

[a] Ferromagnetic state.

Table 4. As table 3 but for Rh, Ir, Cu, Ag and Au.

	χ_0 (10^{-6} emu mol⁻¹)	χ_{so} (10^{-6} emu mol⁻¹)	χ_c (10^{-6} emu mol⁻¹)	$(\chi_c)_{emp}$ (10^{-6} emu mol⁻¹)	$I\chi_s$ (10^{-6} emu mol⁻¹)	χ (10^{-6} emu mol⁻¹)	χ_{exp} (10^{-6} emu mol⁻¹)
Rh	3	6	9	16 [64]	61 [2]	70	102, 106 [69]
				17 [65]	77 [3]	86	
Ir	-18	9	-9		82 [44]	91	27, 35 [69]
					35 [2]	26	
					10 [3]	0	
Cu	-10	0	-10	-14 [66]	10 [26]	0	-5.5 [70]
				-16 [67]	10, 15, 16 [67]	0-6	-5.5 [71]
Ag	-35	0	-35	-43 [66]	10 [3]	-25	-19 [68]
				-39, -42 [68]	9 [26]	-26	-21 [70]
							-20 [71]
Au	-64	2	-62	-62 [66]	10 [26]	-52	-28 [70]
							-28 [71]

and 5d bands, respectively, and their structures are FCC. These metals are neighbours of Ni, Pd and Pt in the periodic table and their band structures are mutually very similar [29, 33, 56–63]. Therefore, it is possible to estimate χ_o and χ_{so} in these metals from table 2 by making reasonable corrections. We can roughly assume the relations $\chi_o \propto a^2/W_d$ and $\chi_{so} \propto a/W_d$ from (1)–(4). If we know a pair of ratios of a and W_d to those of Ni for the 3d series, to those of Pd for the 4d series and to those of Pt for the 5d series, we can estimate more reliable values than those shown in table 2. The two ratios concerning a and W_d are obtained from the data of the lattice constant and the energy difference between self-consistent semi-relativistic X_1 and X_5 levels in a handbook by Papa-constantopoulos [33]. The results are shown in table 4. Agreement between χ_c and $(\chi_c)_{emp}$ is fairly good. By using previously reported theoretical values of $I\chi_s$, the total susceptibility $\chi = I\chi_s + \chi_c$ is estimated and compared with the observed values χ_{exp} in table 4. Agreement between theory and experiment is excellent for Ir and Ag, and satisfactory for Rh, Cu and Au.

4. Conclusion

In this paper, we have evaluated the uniform unenhanced orbital and spin–orbit susceptibilities in Ni, Pd and Pt properly and those in Rh, Ir, Cu, Ag and Au approximately by adopting the rigid-band assumption with reasonable corrections. For both cases, our results are in good agreement with empirical results. For the latter case, theoretical values of the total susceptibility estimated from our results and previously reported theoretical results of the enhanced spin susceptibility are close to observed susceptibilities. Our present study, together with our previous investigations, shows that our numerical method, although simple, is successful in obtaining reliable values of the uniform unenhanced orbital and spin–orbit susceptibilities in transition and noble metals.

Acknowledgments

References

[1] Callaway J and March N H 1984 *Solid State Physics* vol 38 (New York: Academic) p 135
[2] Poulsen U K, Kollár J and Andersen O K 1976 *J. Phys. F: Met. Phys.* **6** L241
[3] Janak J F 1977 *Phys. Rev.* B **16** 255
[4] Liu K L, MacDonald A H, Daams J M, Vosko S H and Koelling D D 1979 *J. Magn. Magn. Mater.* **12** 43
[5] MacDonald A H, Daams J M, Vosko S H and Koelling D D 1981 *Phys. Rev.* B **23** 6377
[6] Yamada H, Yasui M and Shimizu M 1980 *J. Phys. F: Met. Phys.* **10** 913
[7] Callaway J, Chatterjee A K, Singhal S P and Ziegler A 1983 *Phys. Rev.* B **28** 3818
[8] Rajagopal A K and Jain K P 1972 *Int. J. Magn.* **2** 183
[9] Yamada H, Yasui M and Shimizu M 1981 *Physics of Transition Metals 1980 (Inst. Phys. Conf. Ser. 55)* (Bristol: Institute of Physics) p 177

[10] Vignale G, Rasolt M and Geldart D J W 1988 *Phys. Rev.* B **37** 2502
[11] Hebborn J E and Sondheimer E H 1960 *J. Phys. Chem. Solids* **13** 105
[12] Hebborn J E and March N H 1970 *Adv. Phys.* **19** 175
[13] Yasui M and Shimizu M 1979 *J. Phys. F: Met. Phys.* **9** 1653
[14] Yasui M and Shimizu M 1979 *J. Phys. F: Met. Phys.* **9** L227
[15] Yasui M, Yamada H and Shimizu M 1980 *Phys. Lett.* **79A** 439
[16] Yasui M and Shimizu M 1985 *J. Phys. F: Met. Phys.* **15** 2365; 1986 *J. Magn. Magn. Mater.* **54–7** 989
[17] Misra P K and Callaway J 1987 *Phys. Rev.* B **36** 3731
[18] Yasui M 1988 *Physica* B **149** 139
[19] Oh K H, Harmon B N, Liu S H and Sinha S K 1976 *Phys. Rev.* B **14** 1283
[20] Hebborn J E 1960 *PhD Thesis* Queen Mary College, London
[21] Jepsen O and Andersen O K 1971 *Solid State Commun.* **9** 1763
[22] Lehmann G and Taut M 1972 *Phys. Status Solidi* b **54** 469
[23] Lindgård P A 1975 *Solid State Commun.* **16** 481
[24] Rath J and Freeman A J 1975 *Phys. Rev.* B **11** 2109
[25] Janak J F 1974 *Phys. Rev.* B **9** 3985
[26] MacDonald A H, Daams J M, Vosko S H and Koelling D D 1982 *Phys. Rev.* B **25** 713
[27] Wang C S and Callaway J 1977 *Phys. Rev.* B **15** 298
[28] Loucks T L 1967 *Augmented Plane Wave Method* (New York: Benjamin)
[29] Moruzzi V L, Janak J F and Williams A R 1978 *Calculated Electronic Properties of Metals* (New York: Pergamon)
[30] Herman F and Skillman S 1963 *Atomic Structure Calculations* (Englewood Cliffs, NJ: Prentice-Hall)
[31] Christensen N E 1976 *Phys. Rev.* B **13** 2698
[32] Christensen N E 1976 *Phys. Rev.* B **14** 3446
[33] Papaconstantopoulos D A 1986 *Handbook of the Band Structure of Elemental Solids* (New York: Plenum)
[34] Koelling D D and MacDonald A H 1983 *Relativistic Effects in Atoms, Molecules and Solids* (New York: Plenum) p 227
[35] Bacalis N C, Blathras K, Thomaides P and Papaconstantopoulos D A 1985 *Phys. Rev.* B **32** 4849
[36] MacDonald A H 1982 *J. Phys. F: Met. Phys.* **12** 2579
[37] Souletie J and Tholence J L 1983 *Solid State Commun.* **48** 407
[38] Foner S, Freeman A F, Blume N A, Frankel R B, McNiff E J and Praddaude H C 1969 *Phys. Rev.* **181** 863
[39] Rebouillat J P 1972 *IEEE Trans. Magn.* **8** 630
[40] Shimizu M 1970 *Proc. 3rd IMR Symp., Electronic Density of States, National Bureau of Standards Special Publication* p 685
[41] Huguenin R, Pells G P and Baldock D N 1971 *J. Phys. F: Met. Phys.* **1** 281
[42] Jarlborg T and Freeman A J 1981 *Phys. Rev.* B **23** 3577
[43] Stenzel E and Winter H 1985 *J. Phys. F: Met. Phys.* **15** 1571
[44] Cooke J F, Liu S H and Liu A J 1988 *Phys. Rev.* B **37** 289
[45] Stoelinga J H M, Gersdorf R and de Vries G 1969 *Physica* **41** 457
[46] Acker F and Huguenin R 1972 *Phys. Lett.* **38A** 343
[47] Schindler A I and Mackliet C A 1968 *Phys. Rev. Lett.* **20** 15
[48] Chouteau G, Fourneaux R, Gobrecht K and Tournier R 1968 *Phys. Rev. Lett.* **20** 193
[49] Foner S, Doclo R and McNiff E J 1968 *J. Appl. Phys.* **39** 551
[50] Kobayashi S, Launois H, Lederer P, Froideaux C, Treutmann W and Vogt E 1968 *Solid State Commun.* **6** 265
[51] Gerhardt W, Razavi F, Schilling J S, Hüser D and Mydosh J A 1981 *Phys. Rev.* B **24** 6744
[52] Pluzhnikov V and Fawcett E 1982 *J. Phys. F: Met. Phys.* **12** 1467
[53] Ebert H 1988 *Phys. Rev.* B **38** 9390
[54] Krutzen B C H and Springelkamp F 1989 *J. Phys.: Condens. Matter* **1** 8369
[55] Fischer G, Herr A and Meyer A J P 1968 *J. Appl. Phys.* **39** 545
[56] Andersen O K 1970 *Phys. Rev.* B **2** 883
[57] Arbman G O and Hörnfelt S 1972 *J. Phys. F: Met. Phys.* **2** 1033
[58] Smith N V 1974 *Phys. Rev.* B **9** 1365
[59] Smith N V, Wertheim G K, Hüfner S and Traum M M 1974 *Phys. Rev.* B **10** 3197
[60] Mattheiss L F and Dietz R E 1980 *Phys. Rev.* B **22** 1663
[61] Eckardt H, Fritsche L and Noffke J 1984 *J. Phys. F: Met. Phys.* **14** 97
[62] Tripathi G S, Brener N E and Callaway J 1988 *Phys. Rev.* B **38** 10454

[63] Chen H, Brener N E and Callaway J 1989 *Phys. Rev.* B **40** 1443
[64] Shimizu M 1983 *J. Magn. Magn. Mater.* **31–4** 299
[65] Kim D J and Tanaka C 1986 *J. Magn. Magn. Mater.* **58** 254
[66] Takahashi Y and Shimizu M 1971 *J. Phys. Soc. Japan* **31** 1612
[67] Liu K L, MacDonald A H and Vosko S H 1977 *Can. J. Phys.* **55** 1991
[68] Foiles C L 1976 *Phys. Rev.* B **13** 5606
[69] Kojima H, Tebble R S and Williams D E G 1961 *Proc. R. Soc.* A **260** 237
[70] *Landolt–Börnstein New Series* 1962 Group III, vol 9 (Berlin: Springer) p 1
[71] Mendelsohn L B and Biggs F 1970 *Phys. Rev.* A **2** 1130